

Abstract

The Andromeda Galaxy, also known as M31, is very similar to the Milky Way (MW). It has a spiral structure and is comprised of multiple components including a central super-massive black hole, bulge, galactic disk, stellar halo, and circumgalactic medium, all of which have been studied extensively. Furthermore, the Andromeda Galaxy, like all galaxies, is thought to reside within a massive DM halo. The DM halo of M31 is predicted to extend to roughly 300 kpc from its center and have a mass on the order of $10^{12} M_{\odot}$, which amounts to approximately 90% of the galaxy's total mass. For cold DM, the halo is also predicted to contain a large amount of substructure, a subset of which hosts M31's population of satellite dwarf galaxies. The combined M31 system, together with a similar system in the MW, are the primary components of the Local Group. The distance from the MW to M31 is approximately 785 kpc, making it relatively nearby. Consequently, M31 appears extended on the sky. Because of this accessibility, M31 offers a prime target for studying galaxies; and indeed, a wealth of information has been gained from observations in all wavelengths of the electromagnetic spectrum.

Extended γ -ray emission from M31, originating beyond the boundaries of its galactic disk, could arise from cosmic rays (CRs) interacting with the circumgalactic medium and/or stellar halo of M31, or from more exotic processes, such as dark matter (DM) annihilation or decay. We conduct an analysis of 91.4 months of *Fermi*-LAT observations of a 60° radius centered at M31, and we use the CR propagation code GALPROP to construct specialized interstellar emission models to characterize the foreground emission from the MW. Our initial observations are presented. Significant excess emission is detected in the 3–20 GeV energy range, however, important systematic uncertainties remain, the most significant of which pertains to the characterization of atomic hydrogen gas (H I) in the line of sight. Further assessment of these systematics is left for a follow-up study. We discuss the theoretical expectations for a γ -ray signal arising from DM annihilation in M31's outer halo, as well as the corresponding DM halo modeling uncertainties and observational difficulties.

Observations

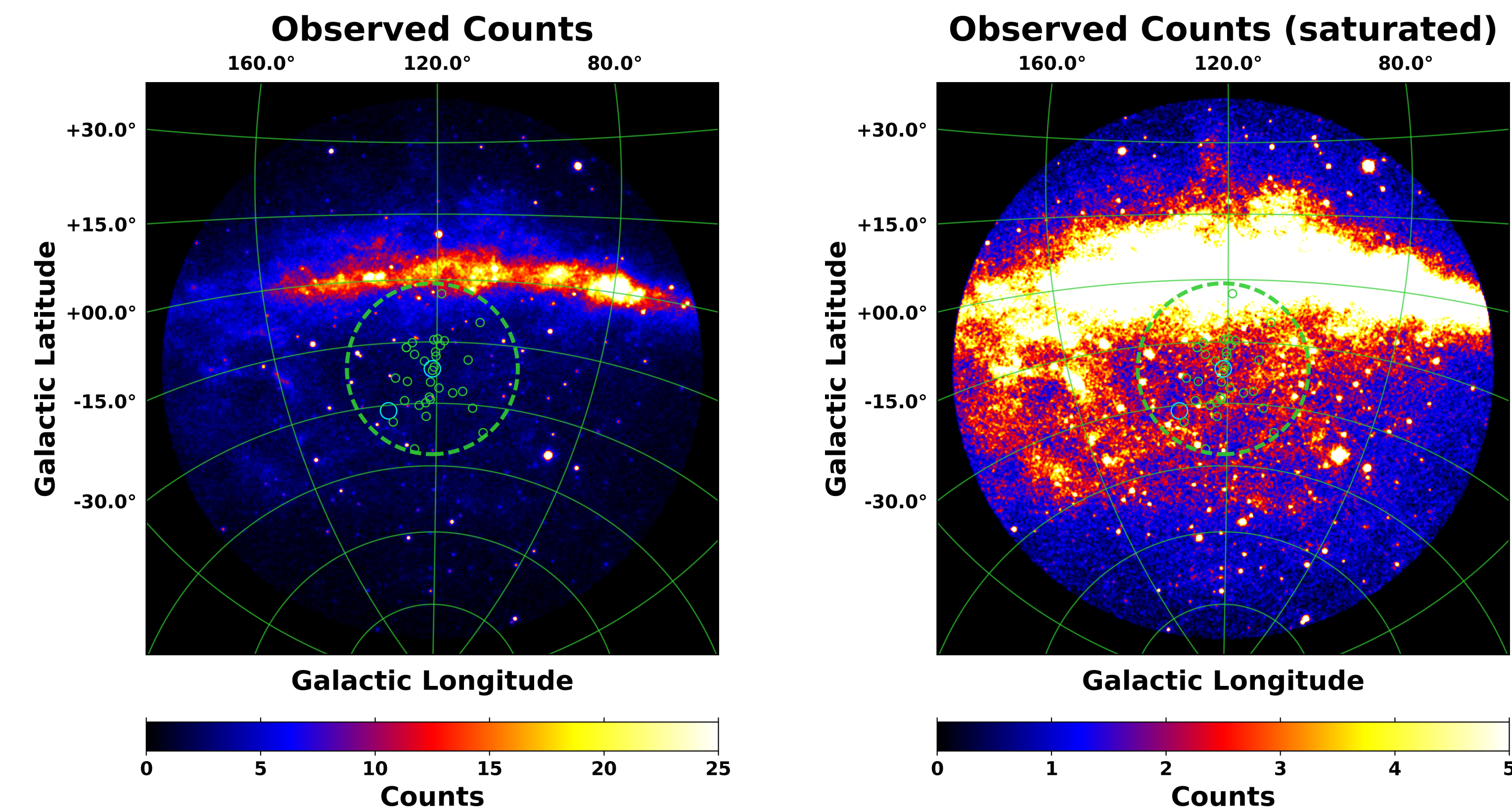


Figure 1: Observed counts (left) and saturated counts (right) for a 60° radius centered at M31. The green dashed circle (21°) corresponds to a 300 kpc projected radius centered at M31, for a MW-M31 distance of 785 kpc, i.e. the canonical virial radius of M31. Also shown is M31's entire population of dwarf galaxies. M31 and M33 are shown with 2° cyan circles, and the other dwarfs are shown with 1° green circles, each centered at the optical center of the respective galaxy. The sizes of the circles are a bit arbitrary, although they roughly correspond to the PSF (68% containment angle) of *Fermi*-LAT, which at 1 GeV is $\sim 1^{\circ}$. Of course the MW dwarfs are not even detected by *Fermi*-LAT, and so we do not expect the individual M31 dwarfs to be detected. The purpose of the overlay is to provide a qualitative representation of the extent of M31's outer halo, and to show its relationship to the MW disk.

Building the IEM with GALPROP

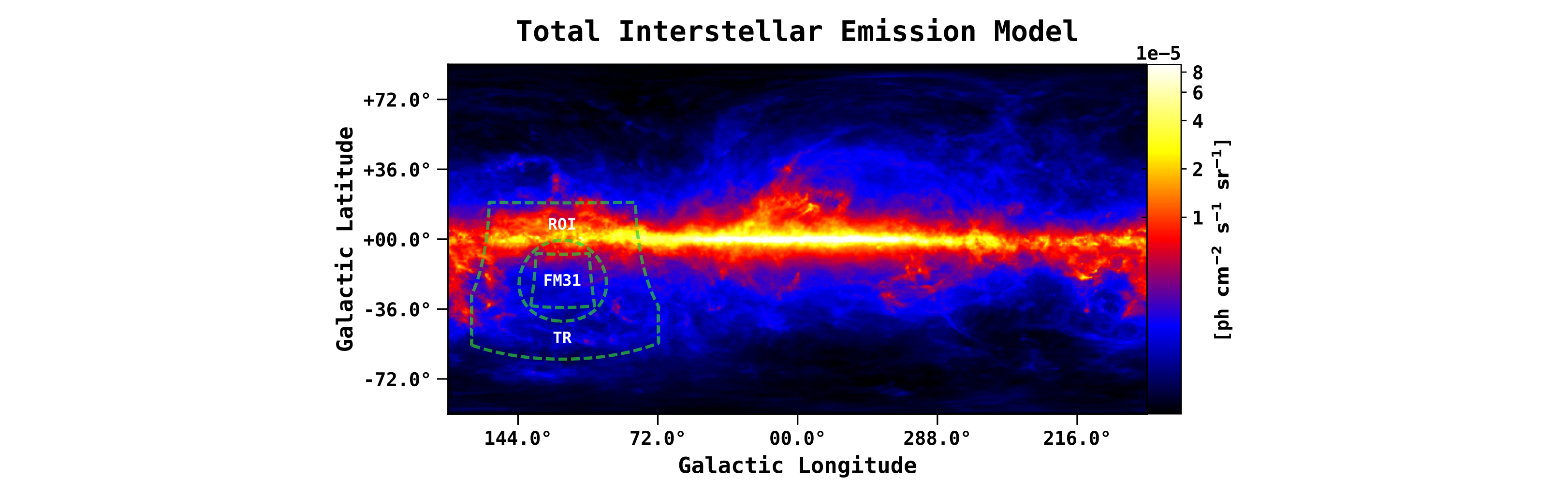


Figure 2: The total interstellar emission model for the MW integrated in the energy range 1–100 GeV. The color corresponds to the intensity, and is shown in logarithmic scale. The intensity level is for the initial GALPROP output, before tuning to the γ -ray data. The map is shown in a Plate Carrée projection, and the pixel size is 0.25 deg/pix. The model has contributions from π^0 -decay, (anisotropic) IC emission, and Bremsstrahlung. From the observed counts (Figure 1) we cut the $84^{\circ} \times 84^{\circ}$ region of interest (ROI), which is centered at M31. The green dashed circle is the 300 kpc boundary corresponding to M31's canonical virial radius. Longitude cuts are made on the ROI at $l = 168^{\circ}$ and $l = 72^{\circ}$. We tune the IC and isotropic components in the tuning region (TR), which is defined by masking the 300 kpc circle and latitudes above -21.5° .

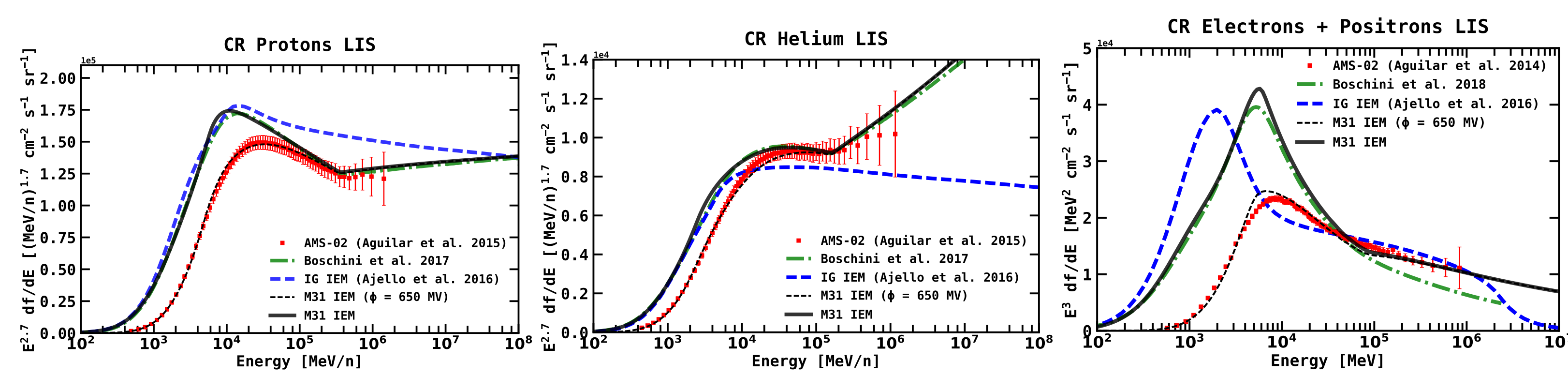


Figure 3: The local interstellar spectra (LIS) for CR protons (left), helium (middle), and electrons + positrons (right). These are fundamental for constructing the γ -ray IEM with GALPROP. The latest AMS-02 measurements are shown with red squares. The green dashed line shows the results from Boschini et al. 2017, 2018, in which GALPROP and HELMOD are used together in an iterative manner to derive the LIS, incorporating solar modulations in a physically motivated way when fitting to the AMS-02 data (along with other CR data sets). We adopt their derived GALPROP CR parameters, and the LIS for our IEM (M31 IEM: solid black line) is roughly the same. For simplicity we modulate our plotted LIS using the force field approximation (thin dotted black line, $\phi = 650$ MV) as a rough comparison to the AMS-02 data below ~ 60 MeV/n, where solar modulations become important. In addition we show the LIS for the IG IEM from Ajello et al. 2016, which we use as a reference model.

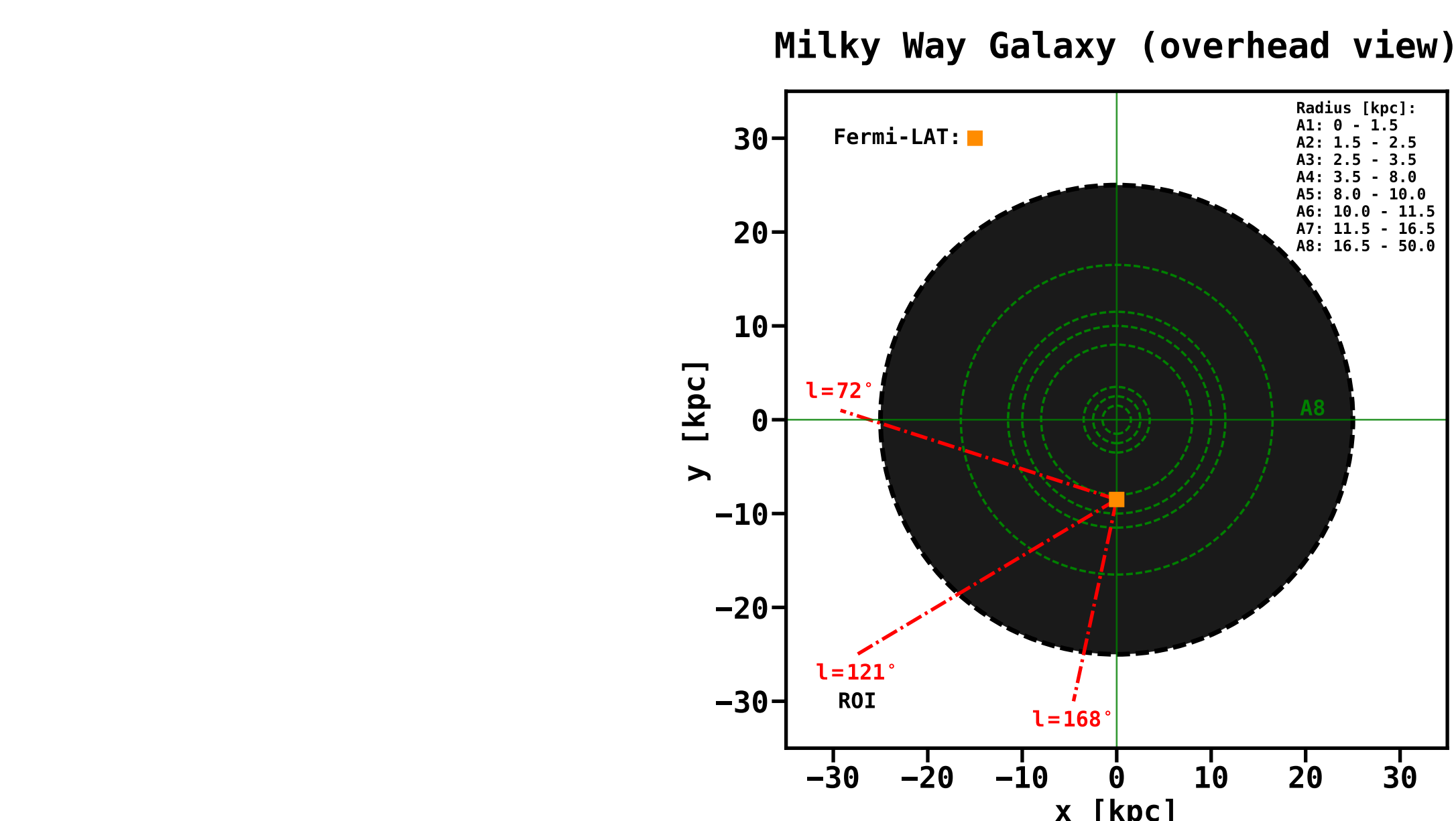


Figure 4: Schematic of the eight concentric circles which define the annuli (A1–A8) in the IEM. The ranges in Galactocentric radii are reported in the legend. Note that the full extension of A8 is not shown. Only A5–A8 contribute to the Galactic foreground emission for the ROI. A longitude cut is made at 168° in order to stay away from the outer Galaxy, where the gas determination becomes more uncertain, due to the method used to assign the gas to Galactocentric radii, i.e. doppler shifted 21 cm emission in accordance with the Galactic rotational curve. The longitude cut at 72° is made to prevent the observations from extending through A4, which would further complicate the analysis due to additional IEM components.

Components of the IEM

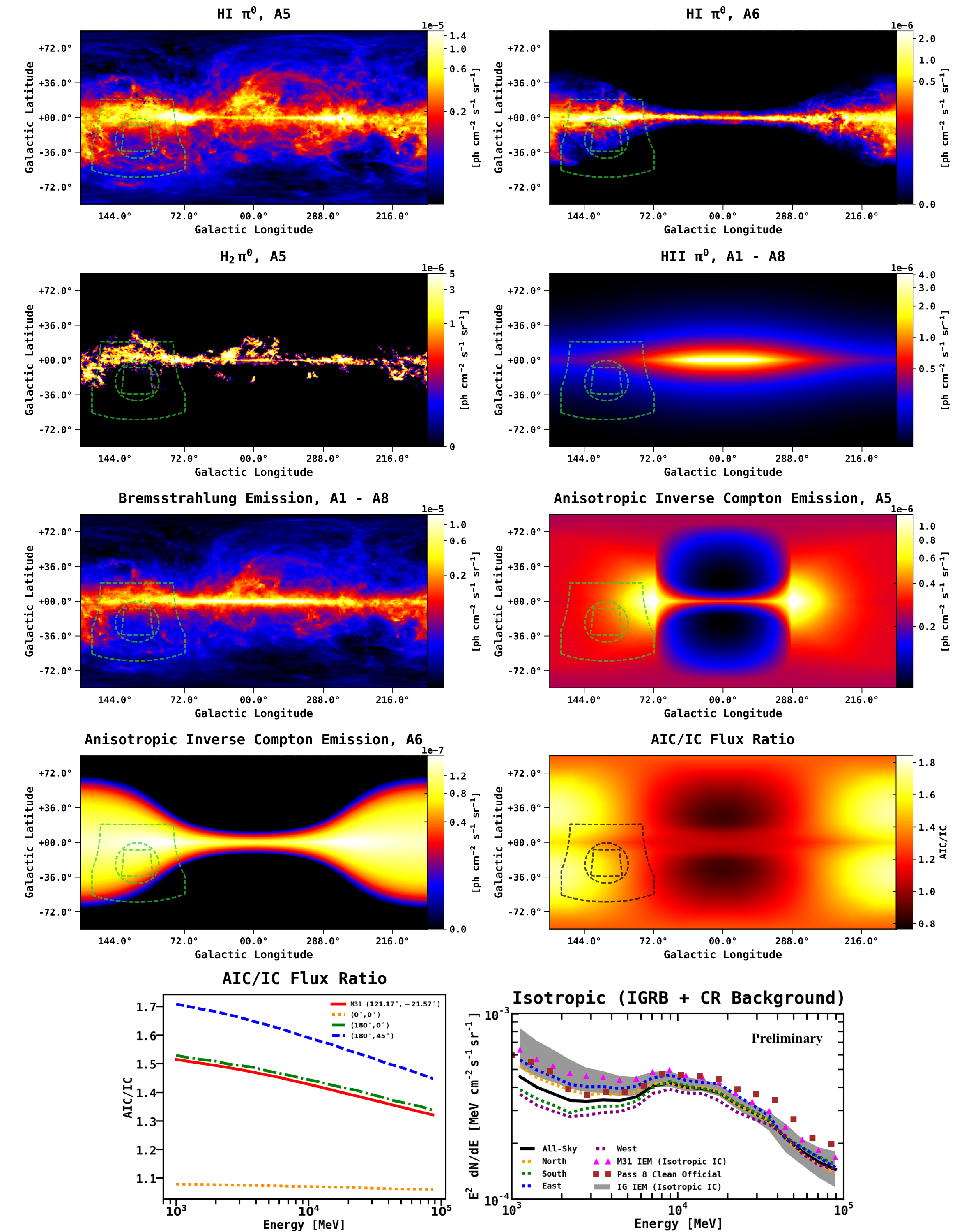


Figure 5: Components of the IEM for the different annuli. We use the anisotropic IC sky maps for our primary IEM. The energy and spatial dependence of the flux ratio (AIC/IC) between the isotropic inverse Compton (IC) and anisotropic inverse Compton (AIC) formalisms are shown. Also shown is our isotropic determination, and the corresponding systematics.

Results

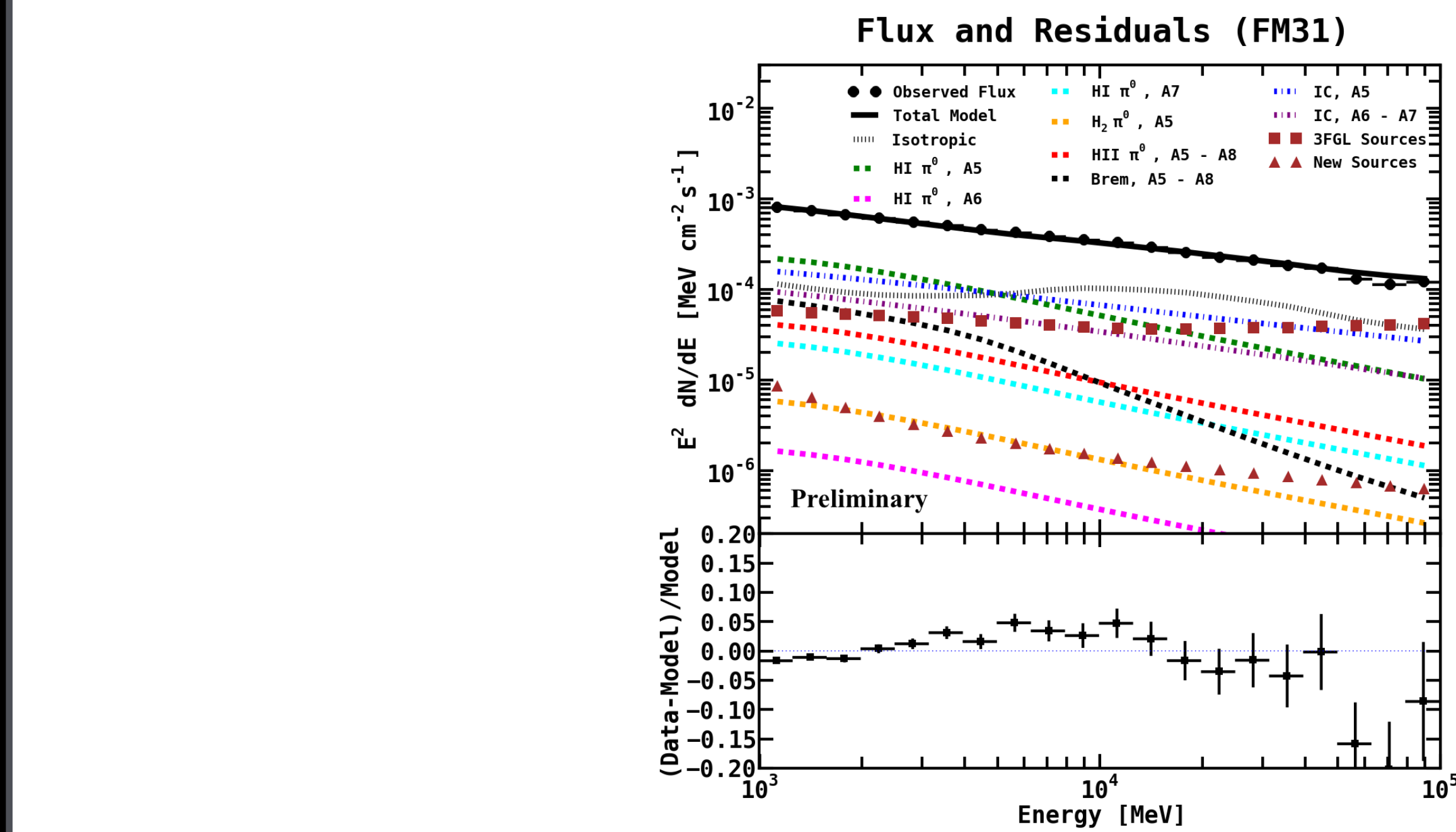


Figure 6: Flux and fractional energy residuals for FM31. The different components are listed in the legend.

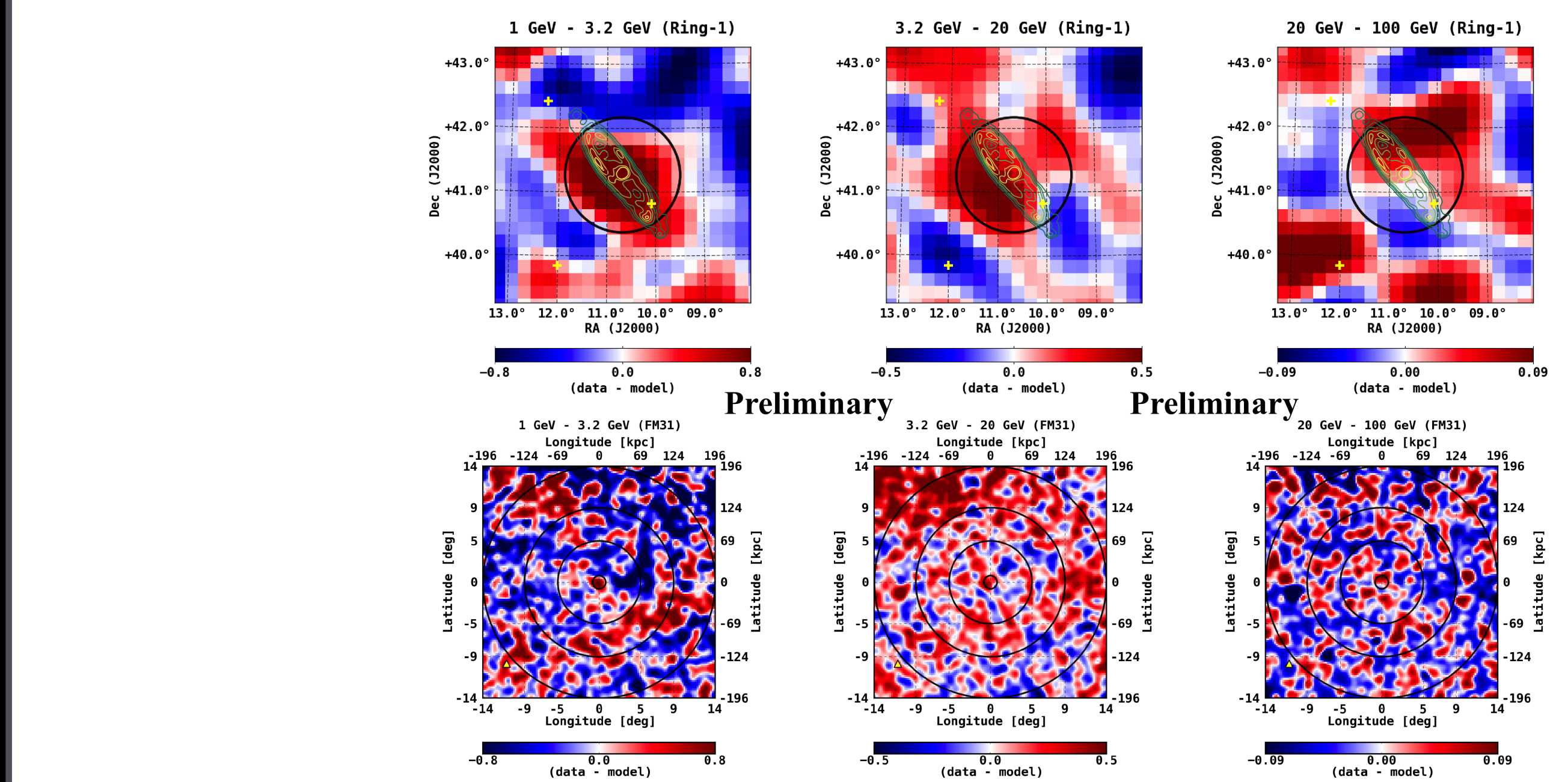


Figure 7: Residual counts map for three different energy bands, as indicated above each plot. The energy bands were chosen to coincide with the observed excess in the fractional residuals. The images are smoothed using a 0.9° Gaussian kernel. The yellow triangle shows the position of M33, for reference. Overlaid are the spatial templates for four concentric rings that are added to the model. *Top row:* Zoomed in to a 2° radius centered at M31. The black circle is the boundary of ring 1 (0.9°). Contours for the IRIS 100 μm map of M31 are overlaid. The IRIS map is smoothed with a 0.5° Gaussian kernel. The levels shown range from 6–22 MJy sr^{-1} . Yellow crosses show 3FGL point sources with $\text{TS} \geq 25$. *Bottom row:* The entire M31 field. Ring 1 is the innermost ring.

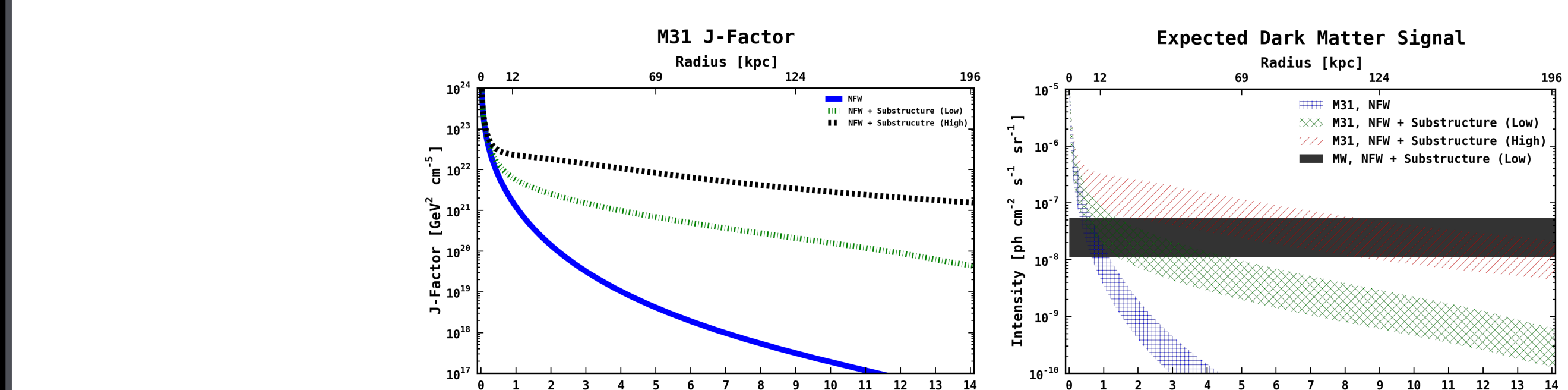


Figure 8: **Left:** Calculated M31 J-factors. The blue solid line shows a smooth NFW halo appropriate for warm DM models that do not produce significant structure below the dwarf galaxy scale. The parameters of the NFW profile are as follows: mass = $10^{12} M_{\odot}$, concentration = 11.2, $R_{\text{virial}} = 210$ kpc, $R_{\text{scale}} = 18.9$ kpc, $\gamma = 1.0$. The green (lower) dashed line, labeled NFW + Substructure (Low), shows the expected DM for a typical ΛCDM cosmology with thermal WIMP DM. For the NFW + Substructure (Low): overall boost factor = 4.2, substructure fraction = 13%, minimum halo mass = $10^{-6} M_{\odot}$. The black (upper) dashed line, labeled NFW + Substructure (High), shows a scenario in which DM is produced very cold such that the minimum mass structures form with very high concentrations. These smallest structures would dominate the annihilation signal. For the NFW + Substructure (High) we use results from Gao et al. 2012. **Right:** The corresponding γ -ray intensity profiles. We use the particle physics constant as determined from the GC excess in Karwin et al. 2016. The uncertainty bands for each of the profiles are due to the uncertainty in the particle physics constant. The model profiles only serve as a representation of the modeling uncertainty associated with M31's DM halo, but they by no means encompass the total modeling uncertainty.